

Teach Diffusion Language Models to Learn from Their Own Mistakes*

Liming Liu, Binxuan Huang, Xin Liu, Bing Yin, Tuo Zhao

January 13, 2026

Abstract

Masked Diffusion Language Models (DLMs) achieve significant speed by generating multiple tokens in parallel. However, this parallel sampling approach, especially when using fewer inference steps, will introduce strong dependency errors and cause quality to deteriorate rapidly as the generation step size grows. As a result, reliable self-correction becomes essential for maintaining high-quality multi-token generation. To address this, we propose **Decoupled Self-Correction (DSC)**, a novel two-stage methodology. DSC first fully optimizes the DLM’s generative ability before freezing the model and training a specialized correction head. This decoupling preserves the model’s peak SFT performance and ensures the generated errors used for correction head training are of higher quality. Additionally, we introduce **Future-Context Augmentation (FCA)** to maximize the correction head’s accuracy. FCA generalizes the error training distribution by augmenting samples with ground-truth tokens, effectively training the head to utilize a richer, future-looking context. This mechanism is used for reliably detecting the subtle errors of the high-fidelity base model. Our DSC framework enables the model, at inference time, to jointly generate and revise tokens, thereby correcting errors introduced by multi-token generation and mitigating error accumulation across steps. Experiments on mathematical reasoning and code generation benchmarks demonstrate that our approach substantially reduces the quality degradation associated with larger generation steps, allowing DLMs to achieve both high generation speed and strong output fidelity.

1 Introduction

Masked Diffusion Models (MDMs) (Sahoo et al., 2024; Shi et al., 2024; Nie et al., 2024) have established themselves as a preeminent paradigm for large language generation, yielding significant speed gains through parallel decoding. The MDM process involves iteratively denoising a corrupted sequence \mathbf{x}_t toward the ground truth \mathbf{x}_0 . However, this parallel generation with only a few inference steps makes them inherently susceptible to dependency errors across positions, as MDMs effectively learn per-position posteriors of the form $p(x_0^{(i)} | \mathbf{x}_t)$ rather than the full joint conditional distribution $p(\mathbf{x}_0 | \mathbf{x}_t) = p(x_0^{(1:N)} | \mathbf{x}_t)$. Consequently, different positions are denoised largely independently, and cross-token dependencies can be systematically violated during parallel decoding.

*Amazon. Correspondence to 11ming@amazon.com

Due to the parallel nature of MDM decoding, dependency errors across positions are more likely to occur (Liu et al., 2024; Xu et al., 2024; Kang et al., 2025). Mistakes made in early denoising steps tend to become fixed and propagate, ultimately degrading global consistency. This vulnerability naturally motivates the need for self-correction mechanisms capable of detecting and rectifying erroneous predictions during inference. To prevent error accumulation, the model must be able to do self-correction, i.e., identify inconsistencies introduced in earlier iterations and revise them in later ones. MDMs inherently support such refinement: at any iteration, a token deemed implausible can be remasked and regenerated using an increasingly coherent surrounding context. This behavior differs fundamentally from autoregressive (AR) models. Although AR models also suffer when early tokens are incorrect, their unidirectional conditioning severely limits error correction. Even if a token were remasked, the model would still condition on the same leftward context that originally produced the error, causing it to regenerate the same high-probability but incorrect token. By contrast, MDMs leverage bidirectional attention and condition on the partially denoised sequence, enabling them to incorporate information from both preceding and subsequent positions when revising a token. This affords MDMs substantially greater flexibility in detecting and correcting errors across iterations, ultimately improving global consistency.

Several previous works have attempted to introduce self-correction mechanism in MDMs (Zhao et al., 2024; Wang et al., 2025; Peng et al., 2025). However, these training-free methods typically rely on inaccurate estimates of token quality, and they cannot be explicitly optimized or explained, which limits their accuracy and general applicability. Recently there are some attempts to introduce trainable self-correction for MDMs (Huang et al., 2025; Kim et al., 2025). These methods rely on joint optimization, simultaneously training the base generator and the self-correction mechanism. While these approaches have demonstrated effectiveness, we observe that jointly optimizing generation and self-correction often leads to a degradation in the base model’s generative capability, suggesting an inherent trade-off between generation quality and correction capacity. Moreover, methods that require simultaneous training of the generator and the self-correction module are difficult to integrate with MDMs that have already undergone extensive post-training, as they necessitate modifying well-optimized model parameters. This requirement further limits their practical impact and applicability, particularly in large-scale or deployment-oriented settings.

1.1 Our Contribution

In this work, we propose a novel two-stage methodology that allows MDMs to self-correct reliably without compromising their core generative fidelity. Our contributions are threefold:

1. We introduce a Decoupled Optimization framework. By fully training the base MDM first, and then freezing the generator to train only the auxiliary correction head, we eliminate the negative interference from dual objectives. This preserves the base model’s integrity and provides a universal, plug-and-play solution.
2. We present a novel training technique, which we term Future-Context Augmentation, that overcomes the error distribution misalignment. By augmenting training samples to simulate

sequences generated with context from a less corrupted state, we enable the correction head to learn how to accurately detect the subtle errors of the fully optimized model.

3. We demonstrate that this approach provides a robust, efficient, and versatile self-correction framework, achieving superior performance across complex MDM generation tasks.

1.2 Concurrent Work

At the end of our project, we notice the concurrent work **PRISM** (Kim et al., 2025) released. **PRISM** (Kim et al., 2025) shares similar motivation with our work, but diverges in optimization strategy and training distribution modeling. We will discuss the detailed difference later.

2 Related Works

Masked Diffusion Models (MDMs) (Sahoo et al., 2024; Gat et al., 2024; Shi et al., 2024) have recently emerged as a compelling alternative to autoregressive models for generative modeling in discrete domains. In contrast to left-to-right generation, MDMs begin inference from a fully masked sequence and iteratively reveal tokens in a non-autoregressive and order-flexible manner until a complete sequence is formed. This ability to unmask tokens in arbitrary orders enables highly parallel generation, which has proven particularly advantageous when combined with recent systems-level and algorithmic advances for large-scale deployment (Nie et al., 2025; Ye et al., 2025; Song et al., 2025; Bie et al., 2025). As a result, MDMs have achieved strong performance across a variety of downstream tasks, including reasoning, coding, and planning, in some cases surpassing their autoregressive counterparts.

A key strength of MDMs lies in their parallel sampling mechanism, which substantially reduces inference latency by completing generation in only a small number of denoising steps. However, this efficiency comes at the cost of weaker modeling of inter-token dependencies (Liu et al., 2024; Xu et al., 2024; Kang et al., 2025). Since MDMs typically estimate per-position unmasking posteriors conditioned on a partially observed sequence—rather than explicitly modeling the full joint distribution over all tokens—they are particularly prone to dependency errors across positions. When multiple tokens are generated or updated simultaneously, inconsistencies can arise and propagate, making the model sensitive to early prediction errors.

These limitations motivate the need for self-correction mechanisms within the MDM framework. Ideally, a generative model should be able to detect low-quality or incorrect predictions and revise them during inference. However, standard MDM formulations lack this capability. Once a masked token is revealed, its value remains fixed for the remainder of the generation process, preventing the model from correcting mistakes introduced in earlier steps. Several previous works have attempted to relax this constraint by introducing remasking or refinement strategies (Zhao et al., 2024; Wang et al., 2025; Peng et al., 2025). However, these training-free methods typically rely on inaccurate estimates of token quality, and they cannot be explicitly optimized or explained, which limits their accuracy and general applicability. Some recent works Huang et al. (2025); Kim et al. (2025) propose some trainable self-correction methods, but they still have some limitations that we will discuss in detail later.

3 Preliminaries

3.1 Masked Diffusion Models

Masked Diffusion Models (MDMs) generate discrete sequences by iteratively denoising partially masked inputs. MDMs consist of a forward corruption process that replaces tokens with a special mask token \mathbb{M} and a reverse process that restores masked tokens given the current partially observed sequence. We then present the training procedure to learn this reverse process and the inference procedure to generate new sequences.

Forward process. Let $\mathbf{x}_0 \in \mathcal{V}^L$ be a length- L clean sequence sampled from dataset \mathcal{D} with vocabulary \mathcal{V} . For time $t \in [0, 1]$, the corrupted sequence $\mathbf{x}_t \in (\mathcal{V} \cup \{\mathbb{M}\})^L$ is sampled by independently masking each position:

$$q_{t|0}(\mathbf{x}_t | \mathbf{x}_0) = \prod_{i=1}^L q_{t|0}(x_t^i | x_0^i), \quad q_{t|0}(x_t^i | x_0^i) = \begin{cases} \alpha_t, & x_t^i = x_0^i, \\ 1 - \alpha_t, & x_t^i = \mathbb{M}. \end{cases}$$

We follow common practice in MDMs to adopt the linear schedule $\alpha_t = 1 - t$. As t increases from 0 to 1, more tokens are masked, until at $t = 1$ the sequence is fully masked.

Reverse process. To generate sequences, we need to reverse this corruption process. The reverse process is defined by reverse transition distributions $\{q_{s|t}(\mathbf{x}_s | \mathbf{x}_t)\}_{0 \leq s < t \leq 1}$ that keep unmasked tokens fixed and only update masked positions. We use the factorization $q_{s|t}(\mathbf{x}_s | \mathbf{x}_t) = \prod_{i=1}^L q_{s|t}(x_s^i | \mathbf{x}_t)$ with

$$q_{s|t}(x_s^i | \mathbf{x}_t) = \begin{cases} \mathbb{1}(x_s^i = x_t^i), & x_t^i \neq \mathbb{M}, \\ \frac{s}{t} \mathbb{1}(x_s^i = \mathbb{M}) + \frac{t-s}{t} q_{0|t}(x_s^i | \mathbf{x}_t), & x_t^i = \mathbb{M}, \end{cases}$$

where $\mathbb{1}(\cdot)$ denotes the indicator function and $q_{0|t}(\cdot | \mathbf{x}_t)$ is the posterior distribution over clean tokens given the masked input \mathbf{x}_t . This posterior is the key quantity we need to learn for generation.

Training. In practice, we parameterize $q_{0|t}(\mathbf{x}_0 | \mathbf{x}_t)$ with a model $p_\theta(\mathbf{x}_0 | \mathbf{x}_t)$ trained to predict original clean tokens from masked inputs. The model parameters θ are learned by minimizing the negative log-likelihood on masked positions. Specifically, we sample $\mathbf{x}_0 \sim \mathcal{D}$ and $t \sim \text{Unif}[0, 1]$, generate $\mathbf{x}_t \sim q_{t|0}(\cdot | \mathbf{x}_0)$, and optimize:

$$\mathcal{L}_{\text{Demask}}(\theta) = \mathbb{E}_{t \sim \text{Unif}[0, 1], \mathbf{x}_0 \sim \mathcal{D}, \mathbf{x}_t \sim q_{t|0}(\cdot | \mathbf{x}_0)} \left[\frac{1}{t} \sum_{i: x_t^i = \mathbb{M}} -\log p_\theta(x_0^i | \mathbf{x}_t) \right] \quad (3.1)$$

We apply the same objective in both pre-training and supervised fine-tuning (SFT) to ensure consistent reconstruction behavior. Once trained, the learned model p_θ is used in place of the true posterior $q_{0|t}$ to define the reverse transitions for generation.

Inference. At generation time, we use the trained model to iteratively unmask a sequence starting from a fully masked sequence $\mathbf{x}_1 = (\mathbb{M}, \dots, \mathbb{M})$. The process proceeds over a decreasing sequence of time steps $t_0 = 1 > \dots > t_N = 0$. At each step ℓ , given the partially masked sequence \mathbf{x}_{t_ℓ} , the transition to $\mathbf{x}_{t_{\ell+1}}$ involves two steps:

1. **Selection:** Identify a subset $\mathcal{S}_\ell \subseteq \{i : \mathbf{x}_{t_\ell}^i = \mathbb{M}\}$ of masked tokens to unmask. Common selection strategies include uniform selection that unmasks a fixed fraction of remaining masks, and confidence-based selection which unmasks the most confident positions under p_θ .
2. **Prediction:** For each position $i \in \mathcal{S}_\ell$, sample the token value $\mathbf{x}_{t_{\ell+1}}^i$ from the model’s predicted distribution $p_\theta(x_0^i | \mathbf{x}_{t_\ell})$.

The parallel update is the main source of speedup in MDM inference. However, this parallelism also induces a structural limitation. Tokens revealed early are predicted under limited context, yet are immediately fixed. Moreover, the parallel generation relies on a product-of-marginals approximation of a joint conditional, which is fragile when token dependencies are strong. Consequently, an early incorrect token can persist to the end and, more importantly, bias subsequent predictions through conditioning, yielding systematic error accumulation along the unmasking trajectory. This motivates a self-correction mechanism that can identify and revise erroneous tokens.

3.2 Self-correction of MDMs

Self-correction enables MDMs to identify and correct likely errors during generation. Existing methods (Huang et al., 2025; Kim et al., 2025) augment the base model with a confidence function $\mathbf{g}_{\theta, \phi}(\mathbf{z}_t)$ that predicts per-token correctness probabilities for a partially masked sequence \mathbf{z}_t , where θ denotes base model parameters and ϕ denotes auxiliary correction head parameters. This confidence function allows the model to remask low-confidence tokens for regeneration in subsequent steps.

This confidence function is $\mathbf{g}_{\theta, \phi}$ trained using Binary Cross-Entropy (BCE) loss to perform per-token binary classification:

$$\mathcal{L}_{Err}(\theta, \phi) = \mathbb{E}_{t \sim \text{Unif}[0,1], \mathbf{x}_0 \sim \mathcal{D}, \mathbf{z}_t} \left[\sum_i \text{BCE}(\mathbf{g}_{\theta, \phi}^i(\mathbf{z}_t), \mathbb{1}[z_t^i = x_0^i]) \right], \quad (3.2)$$

where the indicator function $\mathbb{1}[z_{t,i} = x_{0,i}]$ assigns target 1 to correct tokens and 0 to wrong tokens.

The key design choice is constructing training sequences \mathbf{z}_t with realistic mixtures of correct and incorrect tokens. Prior methods such as **RemeDi** (Huang et al., 2025) and **PRISM** (Kim et al., 2025) start with a corrupted sequence $\mathbf{x}_t \sim q_{t|0}(\cdot | \mathbf{x}_0)$ and introduce “artifact” tokens $\mathbf{y} \sim P_{\text{artifact}}$ at selected positions $\mathcal{M} \subseteq \{i : \mathbf{x}_t^i \neq \mathbb{M}\}$. The training sequence \mathbf{z}_t is generated by

$$\mathbf{z}_t = \text{replace}(\mathbf{x}_t, \mathbf{y}, \mathcal{M}), \quad \text{where} \quad [\text{replace}(\mathbf{x}_t, \mathbf{y}, \mathcal{M})]_i = \begin{cases} y_t^i, & \text{if } i \in \mathcal{M}, \\ x_t^i, & \text{otherwise.} \end{cases}$$

The artifact distribution P_{artifact} and the selection of positions \mathcal{M} together determine which error types the correction head learns to detect, making them crucial design choices. **RemeDi** specifies P_{artifact} as uniform distribution $\text{Unif}(\mathcal{V}^L)$, with \mathcal{M} randomly selected from unmasked positions in \mathbf{x}_t . **PRISM** generates artifacts from the model’s own predictions: given a time step size $\Delta t = 1/N$, it samples a slightly more corrupted state $\mathbf{x}_{t+\Delta t} \sim q_{t+\Delta t|0,t}(\cdot | \mathbf{x}_0, \mathbf{x}_t)$, predicts $\mathbf{y} \sim p_\theta(\mathbf{x}_0 | \mathbf{x}_{t+\Delta t})$, and selects \mathcal{M} from positions that are masked in $\mathbf{x}_{t+\Delta t}$ but unmasked in \mathbf{x}_t , with $|\mathcal{M}| = \lfloor L \cdot \Delta t \rfloor$ to simulate realistic inference errors.

Both methods jointly optimize the base model and correction head parameters:

$$\mathcal{L}(\theta, \phi) = \mathcal{L}_{Demask}(\theta) + \gamma \times L_{Err}(\theta, \phi), \quad (3.3)$$

where γ is a hyperparameter that balances the demasking and error detection objectives. While current methods have shown promising results, we identify several limitations in their training methodology and contextual utilization:

1. **Joint Optimization Challenge.** Jointly training θ and ϕ introduces competing objectives that create a capacity trade-off: the model must allocate resources to both generating high-quality tokens and identifying errors. This dual-objective optimization requires careful tuning of γ to balance generation quality against error detection capability. Moreover, Table 1 demonstrates that this approach can introduce negative interference that degrades the base MDM’s generative fidelity.
2. **Distribution Misalignment.** The effectiveness of the correction head depends critically on whether P_{artifact} matches the errors encountered at inference time. **RemeDi** treats errors as independent random noise and fails to capture the structured, context-dependent errors produced by the trained models. While **PRISM** improves by using model-generated artifacts, it suffers from a training-deployment gap: the correction head is trained to identify errors from the unconverged model θ during joint training. These training-time errors reflect underfitting and optimization instabilities rather than the learned biases and inherent parallel generation difficulties of a fully converged model.
3. **Limited Contextual Exploitation.** A model-generated token may be locally near-optimal given limited context at a particular step, yet globally erroneous. As more tokens are unmasked, such errors often become more apparent. Ideally, the confidence function $\mathbf{g}_{\theta, \phi}$ should leverage this by conditioning on both current and subsequent, more informative states. However, existing methods do not exploit such future context. In **PRISM**, artifacts $\mathbf{y} \sim p_{\theta}(\cdot | \mathbf{x}_{t+\Delta t})$ represent errors made at $t + \Delta t$, which are used to train error detection \mathbf{x}_t . While **PRISM** trains the model to identify its own prediction errors, it restricts error detection to single-step context rather than accumulated context from multiple denoising steps.

4 Method

We propose Decoupled Self-Correction (DSC), a two-stage training framework for masked diffusion language models. To enable effective error detection, we introduce Future-Context Augmentation (FCA), which trains the correction head on sequences that simulate access to future, less-corrupted states. At inference time, we deploy a dynamic remasking mechanism that periodically corrects high-confidence errors identified by the trained correction head. In the sequel, we describe the training procedure in Section 4.1, the augmentation technique in Section 4.2, and the inference algorithm in Section 4.3.

4.1 Decoupled Self-Correction (DSC) Training

We propose DSC, a two-stage training methodology that decouples the optimization of generative quality and error detection capability:

Stage 1: Optimized Generative Training: We fully optimize the base MDM parameters θ using the standard demasking objective $\mathcal{L}_{\text{Demask}}(\theta)$ until achieving a low loss level, obtaining the optimized parameters θ^* .

Stage 2: Specialized Head Training: With θ frozen at θ^* , we train only the correction head parameters ϕ via the Binary Cross-Entropy (BCE) loss:

$$\mathcal{L}_{\text{DSC}}(\phi) = \mathbb{E}_{t \sim \mathcal{U}(0,1), \mathbf{x}_0 \sim \mathcal{D}, \mathbf{z}_t} \left[\sum_i \text{BCE}(\mathbf{g}_{\theta^*, \phi}(\mathbf{z}_t)_i, \mathbb{I}[z_{t,i} = x_{0,i}]) \right], \quad (4.1)$$

where \mathbf{z}_t is generated using Future-Context Augmentation (detailed in Section 4.2).

DSC offers several key advantages. Since Stage 2 optimizes only the correction head ϕ , which constitutes a significantly smaller parameter set relative to the full model, DSC provides a low-cost, plug-and-play solution that can be efficiently integrated into any pre-trained MDM without retraining the base model. Beyond these practical benefits, this decoupled approach directly addresses the first two limitations discussed in Section 3.2:

1. **Preservation of Generative Fidelity.** By freezing θ at θ^* , we prevent the base model from degrading during correction head training, directly addressing the joint optimization challenge. Moreover, the correction head's performance becomes decoupled from the hyperparameter γ in the joint loss (3.3), simplifying training and ensuring stable optimization.
2. **Accurate Error Distribution Alignment:** Training the correction head exclusively on errors generated by the final, fixed θ^* ensures that the correction head ϕ learns to identify the specific errors of the deployed model during inference, addressing the distribution misalignment limitation. This eliminates the training-deployment gap present in joint optimization approaches like PRISM.

4.2 Future-Context Augmentation (FCA)

While DSC addresses the joint optimization challenge and distribution misalignment, addressing the limited contextual exploitation requires augmenting the training data with future context. Ideally, the correction head should learn to leverage not only the current state \mathbf{x}_t but also information from future, less-corrupted states that provide richer context for error detection.

We formalize this through FCA, which constructs the artifact distribution to incorporate future context. Recall that θ^* denotes the frozen parameters from Stage 1 and $\Delta t = 1/N$ is the time step size. For any given time step t and $\mathbf{x}_t \sim q_{t|0}(\cdot|\mathbf{x}_0)$, we construct the artifact sequence \mathbf{y} as follows. We sample $t' \sim \mathcal{U}[\Delta t, 1 - t]$, generate a more corrupted state $\mathbf{x}_{t+t'} \sim q_{t+t'|0,t}(\cdot|\mathbf{x}_0, \mathbf{x}_t)$, and apply the frozen model:

$$\mathbf{y} \sim p_{\theta^*}(\mathbf{x}_0 | \mathbf{x}_{t+t'}).$$

We select a random subset $\mathcal{M} \subseteq \{i : \mathbf{x}_{t+t'}^i = \mathbf{M}\}$ with $|\mathcal{M}| = \lfloor L \cdot \Delta t \rfloor$, and construct the training sequence using $\mathbf{z}_t = \text{replace}(\mathbf{x}_t, \mathbf{y}, \mathcal{M})$.

Intuitively, \mathbf{z}_t simulates realistic errors that originated early in the denoising process and persist to time t . Starting with the relatively clean state \mathbf{x}_t , we corrupt positions in \mathcal{M} with predictions from \mathbf{y} , which was generated from the more corrupted state $\mathbf{x}_{t+t'}$ with limited context. The correction head then learns to identify these persistent errors by exploiting the richer “future” context available at time t , which was unavailable when the errors were originally introduced at $t+t'$. By training on such sequences with varying t' , the correction head ϕ learns robust error detection across different levels of contextual richness.

4.3 Inference with Adaptive Remasking

After training with DSC, we deploy the trained model with parameters (θ^*, ϕ^*) using an inference procedure that corrects errors during generation. Unlike standard MDM generation, which simply applies $p_{\theta^*}(\mathbf{x}_0 | \mathbf{x}_t)$ at each denoising step, our approach strategically remasks erroneous tokens identified by the correction function $\mathbf{g}_{\theta^*, \phi^*}$, allowing the model to regenerate them with richer context in subsequent steps.

The Remasking Strategy: To ensure that the sequence \mathbf{x}_t has information expansion before next remasking step, we introduce a periodic remasking mechanism controlled by a stride parameter d . This prevents premature or over-frequent corrections, allowing the base model θ^* to develop the sequence context over several steps. The remasking process is triggered only at specific time steps t where $t/\Delta t \pmod{d} \equiv d-1$. The detailed mechanism is as follows:

1. **Error Probability Scoring:** At the designated refinement steps, the current intermediate sequence \mathbf{x}_t is passed to the correction head $\mathbf{g}_{\theta^*, \phi^*}$ to compute the per-token error probability:

$$P_{\text{error}}(y_i) = \mathbf{g}_{\theta^*, \phi^*}(\mathbf{x}_t)_i \quad (4.2)$$

2. **Periodic Selection and Thresholding:** The set of indices to be remasked, $\mathcal{M}_{\text{remask}}$, is determined by both temporal and confidence-based constraints:

- **Temporal Trigger:** If $t/\Delta t \pmod{d} \neq d-1$, then $\mathcal{M}_{\text{remask}} = \emptyset$, and the sequence proceeds to step $t-1$ without modification.
- **Refinement Criteria:** If $t/\Delta t \pmod{d} = d-1$, we identify indices i that satisfy:
 - (a) $i \in \text{Top-}K$ indices with the highest $P_{\text{error}}(y_i)$.
 - (b) $P_{\text{error}}(y_i) > \tau$, where τ is a predefined confidence threshold.

3. **Dynamic Sequence Corruption:** For all $i \in \mathcal{M}_{\text{remask}}$, the token y_i in \mathbf{x}_t is replaced with the special [MASK] token. This re-introduces noise into specific low-confidence positions, forcing the base MDM θ^* to re-predict and correct these tokens in the subsequent transition from t to $t - \Delta t$.

Anti-Repetitive Correction Policy: In our practice, we found that a critical issue in iterative self-correction is the risk of oscillatory error correction, where a token is repeatedly predicted as an error and subsequently re-generated identically by the MDM. This wastes remasking capacity and stalls the generation process. To address this, we implement an **Anti-Repetitive Correction Policy**. We maintain a memory $\mathcal{H}_{\text{block}}$ of the indices that have been remasked in the recent few steps. Tokens whose indices are present in $\mathcal{H}_{\text{block}}$ are temporarily prohibited from being remasked again. This strategy ensures that the self-correction mechanism prioritizes exploration of new error locations, preventing cycles and optimizing the utilization of the limited remasking budget.

We summarize our inference techniques and show the specific algorithm in Algorithm 1.

Algorithm 1 Dynamic Self-Correction Inference with Bounded Block Buffer

Require: Generative model θ^* , Correction head ϕ^* , Total steps T , Confidence threshold τ , Max remask tokens K , Self-correction stride d , Block buffer capacity B .

```

1:  $\Delta t \leftarrow \frac{1}{T}$ ,  $k \leftarrow \lfloor \Delta t \times L \rfloor$ 
2: Initialize:  $\mathbf{x}_1 \leftarrow [\text{MASK}]^L$ ,  $\mathcal{H}_{\text{block}} \leftarrow \emptyset$  (queue)
3: for  $N = 0 \rightarrow T - 1$  do
4:    $t \leftarrow 1 - \frac{N}{T}$ 
5:    $P_{\text{demask}} \leftarrow p_{\theta^*}(\mathbf{x}_{t-\Delta t} \mid \mathbf{x}_t)$ 
6:    $\mathcal{I} \leftarrow \text{arg-top-}k(P_{\text{demask}})$ 
7:   Sample  $\mathbf{x}_{t-\Delta t}[i] \sim P_{\text{demask}}[i]$  for all  $i \in \mathcal{I}$ 
8:   if  $N \bmod d = d - 1$  then
9:      $P_{\text{error}} \leftarrow \mathbf{g}_{\theta^*, \phi^*}(\mathbf{x}_t)$ 
10:     $\mathcal{M}_{\text{candid}} \leftarrow \text{arg-top-}K(P_{\text{error}})$ 
11:     $\mathcal{M}_{\text{remask}} \leftarrow \emptyset$ 
12:    for index  $i$  in  $\mathcal{M}_{\text{candid}}$  do
13:      if  $P_{\text{error}}(i) > \tau$  and  $i \notin \mathcal{H}_{\text{block}}$  then
14:        Add  $i$  to  $\mathcal{M}_{\text{remask}}$ 
15:      end if
16:    end for
17:    for index  $i$  in  $\mathcal{M}_{\text{remask}}$  do
18:       $\mathbf{x}_{t-\Delta t}[i] \leftarrow [\text{MASK}]$ 
19:      if  $|\mathcal{H}_{\text{block}}| \geq B$  then
20:        Remove the oldest element from  $\mathcal{H}_{\text{block}}$ 
21:      end if
22:      Append  $i$  to  $\mathcal{H}_{\text{block}}$ 
23:    end for
24:  end if
25: end for

```

5 Experiments

5.1 SMDM Fine-Tuning Setting

5.1.1 Architecture and Implementation Details

To realize the Decoupled Self-Correction (DSC) framework, we adopt an architectural design inspired by **RemeDi**. Specifically, we leverage the deep semantic representations of the backbone by extracting the output of the *31st* transformer block of LLaDA as the input to the correction head ϕ . The correction head ϕ is designed as a lightweight yet expressive module, consisting of **three layers of standard Transformer attention blocks**. By extracting features from the penultimate layers of the frozen MDM θ^* , the head benefits from high-level contextual embeddings while remaining computationally efficient.

We test our Decoupled Self-Correction (DSC) framework and compare it against the SFT_{Base} and a Joint Optimization approach (similar to PRISM), where the correction head ϕ and the base MDM θ are trained simultaneously. The core metric is the final generation accuracy (acc) on the GSM8K test set. For all methods, we set the number of tokens generated per step to 2 during inference. Remasking selection number K and remasking stride d in Algorithm 1 are also 2.

5.1.2 Results on Generative Fidelity

We systematically compare the generative performance of three models under two conditions: standard generation (no self-correction applied) and generation with remasking (self-correction applied).

Table 1: Comparison of Generative Accuracy on GSM8K Test Set (%).

Method	Acc. (No Remask)	Acc. (With Remask / DSC Applied)
SFT (Baseline, θ^*)	61.33	--
Joint Optimization (Simultaneous $\theta + \phi$)	60.56	62.62
DSC (Decoupled θ^* , then ϕ)	61.33	63.46

The results in Table 1 highlight the critical trade-offs in optimization:

- **Generative Degradation with Joint Optimization:** When the correction head is trained simultaneously with the base MDM (Joint Optimization), the model’s intrinsic generative fidelity suffers significantly. The accuracy without applying remasking drops to 65.2%, indicating that the dual objective optimization has compromised the model’s core generative capability (\mathcal{L}_{SFT}).
- **Decoupled Training Preserves Fidelity:** In contrast, the DSC method, which freezes θ at θ^* before training ϕ , successfully preserves the generative integrity of the base model. Its performance without remasking remains at the SFT_{Base} level (60.56%). This empirically

validates our core hypothesis that decoupled training eliminates the negative interference of joint optimization.

- **Superior Performance with Correction:** When the self-correction mechanism (via remasking) is applied, both methods improve significantly over the SFT_{Base}. However, DSC consistently **outperforms** Joint Optimization (63.46% vs. 62.62%). This demonstrates that starting from an optimally tuned θ^* and training the correction head on a more aligned error distribution yields a more powerful and accurate self-correction mechanism.

5.2 Experiments on LLaDA 8B

To rigorously evaluate the efficiency and performance of our Decoupled Self-Correction (DSC) framework, we conduct experiments across two critical domains: **Coding** and **Mathematical Reasoning (Math)**. Our base model for all experiments is the LLaDA 8B model ([Nie et al., 2025](#)).

5.2.1 Coding Experiments

We first establish a strong generative baseline for the coding domain. The LLaDA 8B base model is Supervised Fine-Tuned (SFT) on the first 500,000 samples from the OpenCodeInstruct ([Ahmad et al., 2025](#)) dataset. This results in our baseline model. Following the fine-tuning of the base model, the correction head ϕ of our DSC framework is subsequently trained on the same 500,000 OpenCodeInstruct samples for a single epoch.

We evaluate the performance of our DSC approach against the SFT baseline on the MBPP and HumanEval benchmarks. The key metrics are: Acc (Pass@1) and the Average Generation Iterations (Iter_{avg}) on the bechmark.

For the LLaDA base model, we employ semi-autoregressive generation protocol: a block length of 32 tokens and a maximum total generation length of 1024 tokens. Crucially, after the generation of each block, we implement **early stopping** upon detecting the End-of-Sequence token. All reported Iter_{avg} values for both methods adhere to this early-stopping protocol to ensure a meaningful comparison of efficiency. We observed that, for all methods, increasing the number of tokens generated per step leads to a decrease in the average inference iterations but is accompanied by a degradation in accuracy, which is consistent with the observation reported in LLaDA paper.

Table 2 summarizes the comparative results on the MBPP benchmark. Table 3 summarizes the comparative results on the HumanEval benchmark.

Table 2: Comparative results with SFT on the MBPP benchmark.

Method	k (Tokens/Step)	Acc (Pass@1) (%)	Iter _{avg} (Steps)
SFT (Baseline)	1	39.8	119.4
	2	35.6	59.3
	3	30.4	44.3
	4	24.6	30.0
Our Method	1	40.2	134.0
	2	40	69.6
	3	35.6	45.6
	4	33.8	35.9

Table 3: Comparative results with SFT on the HumanEval benchmark.

Method	k (Tokens/Step)	Acc (Pass@1) (%)	Iter _{avg} (Steps)
SFT (Baseline)	1	35.98	131.0
	2	28.66	67.1
	3	24.39	41.5
	4	20.73	29.2
Our Method	1	36.59	138.6
	2	33.54	71.1
	3	33.29	41.5
	4	27.44	35.5

5.2.2 Mathematical Reasoning Experiments

The setup for the Math domain experiments is analogous to the Coding setup. The LLaDA 8B base model is SFT on the first 500,000 samples from openmathinstruct (Toshniwal et al., 2024). The correction head is trained on the same data. We evaluate the performance on GSM8k and Math. The comparison between DSC and the baseline, including the Iter_{avg} calculation, strictly adheres to the same **early-stopping** semi-autoregressive protocol.

Table 4 summarizes the comparative results on GSM8K. Table 5 summarizes the comparative results on Math.

Table 4: Comparative results with SFT on the GSM8K benchmark.

Method	k (Tokens/Step)	Acc (Pass@1) (%)	Iter_{avg} (Steps)
SFT (Baseline)	1	75.44	159.8
	2	70.28	77.9
	3	61.26	52.3
	4	56.18	39.8
	5	47.69	36.8
Our Method	1	76.72	245.6
	2	74.30	109.1
	3	70.81	65.7
	4	67.48	50.4
	5	59.51	39.6

Table 5: Comparative results with SFT on the Math benchmark.

Method	k (Tokens/Step)	Acc (Pass@1) (%)	Iter_{avg} (Steps)
SFT (Baseline)	1	34.2	190.5
	2	31.6	85.3
	3	28.4	61.1
	4	22.4	47.1
Our Method	1	36.2	324.42
	2	34	127.9
	3	33.6	75.4
	4	28.4	56.1

We also plotted the relationship between average iteration and accuracy in figure 1 to demonstrate how our method expands the Pareto frontier compared to the baseline and other methods.

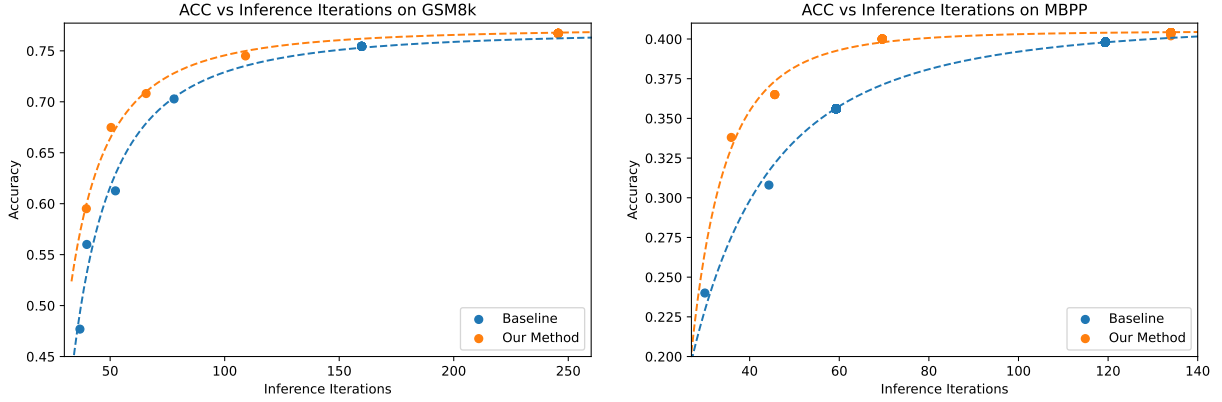


Figure 1: The accuracy vs. iterations comparison between our method and baseline SFT on GSM8k and MBPP. Data is from Table 2 and Table 4. Our methods is Pareto better than baseline.

5.3 Ablation on the artifact distribution

To further illustrate how the quality of artifact distribution impacts the capability of the self-correction head, we conducted the following ablation study: while maintaining the Decoupled Self-Correction (DSC) framework, we replaced the P_{artifact} in FCA with a uniform distribution, consistent with the one used in RemeDi. Subsequently, we re-evaluated this configuration on GSM8k with the setting of LLaDA 8B discussed in Section 5.2 and compared the results against our proposed method. See the results in Table 6.

Table 6: Comparative results with ablation method on the GSM8K benchmark.

Method	k (Tokens/Step)	Acc (Pass@1) (%)	Iter _{avg} (Steps)
Ablation	1	75.74	158.1
	2	70.74	78.6
	3	63.61	52.7
	4	58.38	40.5
	5	49.37	36.4
Our Method	1	76.72	245.6
	2	74.30	109.1
	3	70.81	65.7
	4	67.48	50.4
	5	59.51	39.6

We plot the results in Figure 2 to show that our method is Pareto better.

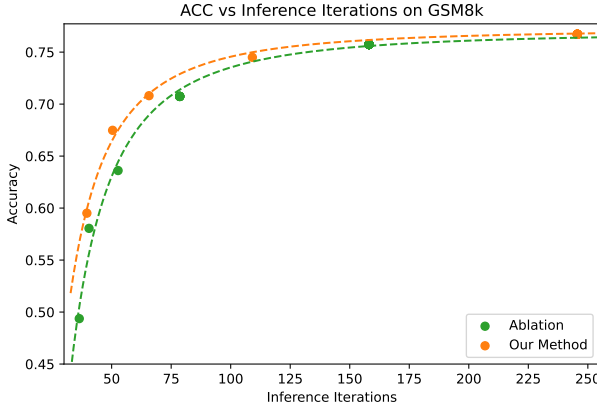


Figure 2: The accuracy vs. iterations comparison between our method and the ablation method in Section 5.3 on GSM8k and MBPP. Data is from Table 6. Our methods is Pareto better than the ablation method.

5.4 Comparison with randomly remasking

We also compare our method with random remasking methods proposed in Wang et al. (2025). Since we use Semi-autoregressive method to generate the response and use early stopping strategy to save the inference time, there isn't a standard time schedule for the generation as in Wang et al. (2025). Instead, we just adjust P_{error} in our inference method (Algorithm 1) to be a random probability in $U[0, 1]$. Thus in every remasking iteration the remasking tokens are randomly selected.

We found that although randomly remasking tokens can improve final accuracy over the baseline SFT, it fails to reliably identify erroneous tokens. As a result, tokens are remasked excessively, leading to a large number of inference iterations.

We compare our method with such randomly remasking method on GSM8K, as shown in Table 7. We also plot the results in Figure 3 to show that our method is Pareto better than randomly remasking.

6 Conclusion

In this paper, we propose a novel self-correction framework. By **decoupling** the training of the MDM and the correction head, we first establish a high-fidelity generative base through SFT, subsequently training the correction head to focus exclusively on the nuanced errors produced by the optimized model. This ensures that the training distribution is precisely aligned with the actual distribution encountered during inference. Furthermore, we introduce **Future-Context Augmentation (FCA)**, which enables the model to leverage expanded future information to identify previously undetected errors. Our method aims to synchronize the self-correction objectives with actual inference demands, and significantly improves the robustness and generative integrity of diffusion models on different benchmarks.

Table 7: Comparative results with random remasking method on the GSM8K benchmark.

Method	k (Tokens/Step)	Acc (Pass@1) (%)	Iter _{avg} (Steps)
Random Remask	1	75.82	338.4
	2	71.95	155.6
	3	66.64	75.3
	4	63.08	58.7
	5	51.10	40.9
Our Method	1	76.72	245.6
	2	74.30	109.1
	3	70.81	65.7
	4	67.48	50.4
	5	59.51	39.6

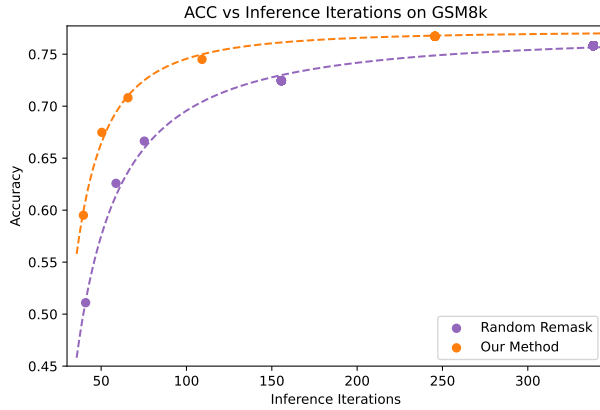


Figure 3: The accuracy vs. iterations comparison between our method and randomly remasking method in Section 5.4 on GSM8k. Data is from Table 7. Our methods is Pareto better than the ablation method.

References

AHMAD, W. U., FICEK, A., SAMADI, M., HUANG, J., NOROOZI, V., MAJUMDAR, S. and GINSBURG, B. (2025). Opencodeinstruct: A large-scale instruction tuning dataset for code llms. *arXiv preprint arXiv:2504.04030*.

BIE, T., CAO, M., CHEN, K., DU, L., GONG, M., GONG, Z., GU, Y., HU, J., HUANG, Z., LAN, Z. ET AL. (2025). Llada2. 0: Scaling up diffusion language models to 100b. *arXiv preprint arXiv:2512.15745*.

GAT, I., REMEZ, T., SHAUL, N., KREUK, F., CHEN, R. T., SYNNAEVE, G., ADI, Y. and LIPMAN, Y. (2024). Discrete flow matching. *Advances in Neural Information Processing Systems*, 37 133345–133385.

HUANG, Z., WANG, Y., CHEN, Z. and QI, G.-J. (2025). Don't settle too early: Self-reflective remasking for diffusion language models. *arXiv preprint arXiv:2509.23653*.

KANG, W., GALIM, K., OH, S., LEE, M., ZENG, Y., ZHANG, S., HOOPER, C., HU, Y., KOO, H. I., CHO, N. I. ET AL. (2025). Parallelbench: Understanding the trade-offs of parallel decoding in diffusion llms. *arXiv preprint arXiv:2510.04767*.

KIM, J., KIM, S., LEE, T., PAN, D. Z., KIM, H., KAKADE, S. and CHEN, S. (2025). Fine-tuning masked diffusion for provable self-correction. *arXiv preprint arXiv:2510.01384*.

LIU, A., BROADRICK, O., NIEPERT, M. and BROECK, G. V. D. (2024). Discrete copula diffusion. *arXiv preprint arXiv:2410.01949*.

NIE, S., ZHU, F., DU, C., PANG, T., LIU, Q., ZENG, G., LIN, M. and LI, C. (2024). Scaling up masked diffusion models on text. *arXiv preprint arXiv:2410.18514*.

NIE, S., ZHU, F., YOU, Z., ZHANG, X., OU, J., HU, J., ZHOU, J., LIN, Y., WEN, J.-R. and LI, C. (2025). Large language diffusion models. *arXiv preprint arXiv:2502.09992*.

PENG, F. Z., BEZEMEK, Z., PATEL, S., RECTOR-BROOKS, J., YAO, S., BOSE, A. J., TONG, A. and CHATTERJEE, P. (2025). Path planning for masked diffusion model sampling. *arXiv preprint arXiv:2502.03540*.

SAHOO, S., ARRIOLA, M., SCHIFF, Y., GOKASLAN, A., MARROQUIN, E., CHIU, J., RUSH, A. and KULESHOV, V. (2024). Simple and effective masked diffusion language models. *Advances in Neural Information Processing Systems*, 37 130136–130184.

SHI, J., HAN, K., WANG, Z., DOUCET, A. and TITSIAS, M. (2024). Simplified and generalized masked diffusion for discrete data. *Advances in neural information processing systems*, 37 103131–103167.

SONG, Y., ZHANG, Z., LUO, C., GAO, P., XIA, F., LUO, H., LI, Z., YANG, Y., YU, H., QU, X. ET AL. (2025). Seed diffusion: A large-scale diffusion language model with high-speed inference. *arXiv preprint arXiv:2508.02193*.

TOSHNIWAL, S., DU, W., MOSHKOV, I., KISACANIN, B., AYRAPETYAN, A. and GITMAN, I. (2024). Openmathinstruct-2: Accelerating ai for math with massive open-source instruction data. *arXiv preprint arXiv:2410.01560*.

WANG, G., SCHIFF, Y., SAHOO, S. S. and KULESHOV, V. (2025). Remasking discrete diffusion models with inference-time scaling. *arXiv preprint arXiv:2503.00307*.

XU, M., GEFFNER, T., KREIS, K., NIE, W., XU, Y., LESKOVEC, J., ERMON, S. and VAHDAT, A. (2024). Energy-based diffusion language models for text generation. *arXiv preprint arXiv:2410.21357*.

YE, J., XIE, Z., ZHENG, L., GAO, J., WU, Z., JIANG, X., LI, Z. and KONG, L. (2025). Dream 7b: Diffusion large language models. *arXiv preprint arXiv:2508.15487*.

ZHAO, Y., SHI, J., CHEN, F., DRUCKMANN, S., MACKEY, L. and LINDERMAN, S. (2024). Informed correctors for discrete diffusion models. *arXiv preprint arXiv:2407.21243*.

A Training Details of DSC on LLaDA 8B

As introduced in Section 4, the training of DSC is divided into two components: standard SFT training and the training of the self-correction head. We describe the details of these two components separately below.

A.1 Supervised Finetuning (SFT)

Our SFT stage basically follow the method propised in LLaDA (Nie et al., 2025). We set the maximum length to be 1024 and use the special token “End-of-Sentecne”([EoS]) to pad all the data to be the maximum length. Data exceeds the max length will be discarded.

In LLaDA (Nie et al., 2025), these padding [EoS] tokens are treated as normal tokens, which means that they will be also randomly masked with the same probability as tokens in the response. However, if the majority data are much shorter than the max length, there will be too many [EoS] tokens in the final padded data, and the model learn to predict [EoS] with a high probability. The result is that the model will tend to end the response early even though the response is not completed. We note that LLaDA (Nie et al., 2025) also report this issue for their finetuned instruct model in their github.

To address this issue, we make a very small but effective modification during the SFT stage. We still treat the first 16 [EoS] tokens as normal tokens, which means these tokens may still be masked. For the other [EoS] padding tokens, we just keep them to be unmasked. This method will effectively constrain the number of [EoS] tokens that need to be predicted in the SFT data. We found that this method effectively address the issue that the model tends to predict [EoS] token and end the response.

Finally we use the standard SFT loss for diffusion LLM as in Equation (3.1) to train the base model. We train LLaDA 8B Base on Opencodeinstruct (Ahmad et al., 2025) and Openmathinstruct(Toshniwal et al., 2024) respectively and test the finetuned model on Coding and Math benchmarks correspondingly.

A.2 Training of the self-correction head

The training of the self-correction head is after the SFT stage, and the parameter of the MDM θ^* is well optimized. Then we use a transformer block ϕ with two layers to be self correction head. The correction head ϕ takes the output of the 31st layer of the MDM to be the input, and it outputs a probability to predict whether the token is true or wrong. The correction head ϕ has only 100M parameters, so the training of ϕ is very light weight. The training method is introduced in Section 4.1 and Section 4.2. Training dataset for head ϕ is completely same as that for θ^* . Therefore, The two stage training doesn’t introduce any new data.

Same as the trick in Section A.1, we treat the first 16 [EoS] tokens as normal tokens, and keep the other [EoS] padding tokens to be unmasked during the generate process of \mathbf{z}_t in Equation (4.1).